



Effect of Plating Materials on the Corrosion Properties of Steel Alloy 4130



A. M. El-Shamy^{a*}, Y. Reda^b, K. M. Zohdy^c, and Ashraf K. Eessaa^d

^{a*} Physical Chemistry Department, Electrochemistry and Corrosion Lab., National Research Centre, El-Bohouth St. 33, Dokki, P.O. 12622, Giza, ^t ^b Chemical Engineering Department, Higher Institute of Engineering and Technology New Damietta, ^c Higher Technological Institute, 10th of Ramadan City and ^d Electronic Research Institute, Lab. of Nanotechnology, Egypt

The corrosion behavior of uncoated and Ni, Cu and Cd coated steel alloy 4130 in 3.5 wt. % NaCl solution was anticipated. The Ni-coated sample showed greater corrosion inhibition effect than both Cu-coated and Cd-coated depending on the obtained results of open circuit potential, polarization curves, impedance spectroscopy and cyclic voltammetry. The surfaces of uncoated and coated samples are characterized by scanning electron microscopy before and after immersion in salt solution. The best corrosion resistance and surface morphology achieved in Ni-coated steel alloy. The inhibition efficiencies of tested samples were 90.7, 89.1 and 56.9 for the Ni-coated, Cu-coated and Cd-coated respectively.

Keyword: Steel Alloy 4130; Electroplating; Polarization; EIS; SEM

1. Introduction

Because of higher tensile strength and lower cost of steel alloys, it was widely applied in infra structure of many industrial companies [1-5]. The alloying elements such as carbon and other elements are controlling the physical and mechanical properties [6-8]. However, the plain iron carbon alloys have carbon content in steel alloy ranged from 0.002% to 2.1% by weight. The steel 4130 has carbon concentrations ranged from 0.25% to 0.60% wt. %, so it is considered as medium-carbon steel [9-11]. The mechanical properties of this alloy can be improved by heat treatment

[12]. The capacity and strength ductility of these alloys can be achieved by adding some elements such as chromium, nickel, and molybdenum [13-16]. To assure about the infrastructures in industrial manufactures to spend long time without any deterioration or degradation of steel alloy, the protection of metallic structures from corrosion is necessity. The corrosion process is identified as the degradation or deterioration of metallic materials by interaction between the metal surface and the environment [17-19]. The corrosion process is a natural process because the elements or metals tend towards the lowest

*Corresponding author e-mail: elshamy10@yahoo.com

Received 22/3/2019; Accepted 7/7/2019

DOI: 10.21608/ejchem.2019.11023.1706

©2020 National Information and Documentation Center (NIDOC)

energy states [20-23]. However, the steel has a tendency to react with specific elements to come back to its lowest energy states. The probable environmental corrosion reactions are the reaction of steel with O₂ and/or H₂O to form hydrated iron oxides, which constitute the chemical structure of the original iron ore [24-25]. The electroplating process is one of the best methods of corrosion protection; however, it is used to improve the multitalented process of surface finishing for broad-spectrum applications [26-27]. The technique is depending on formation of thin layer on the metal surface. However, the applications of this process include; decorative, functional, and electroforming [28-30]. In decorative part, the nickel combined with chromium to prevent the tarnishing of nickel. In our study, the nickel coatings are widely specified to protect materials from severe corrosive media [31-32]. The nickel coatings are able to protect steel, zinc, copper and aluminum from corrosion for extended periods without increasing the thickness and costs. Our works are depending on the plating of the steel alloy 4130 with different types of plating (cadmium-nickel-copper), and study the effect of plating on the corrosion properties of steel alloy. This alloy is used in the aircraft industry as previously mentioned. The study is focused on the discussion of the effect of electroplating techniques on the prevention or control of corrosion of this alloy. Here is the novelty of this study because there is no similar study on this alloy are previously discussed. In this paper the study is focused on

the effectiveness of electroplating process on the resistance to general corrosion.

2. Materials and Methods

2.1. Materials

The material used in this investigation was 4130 steel alloy and Table 1 represents the chemical analysis of this alloy.

Table 1. Chemical analysis of steel alloy 4130.

2.2. Methods

2.2.1. Electroplating Technique

The physical embodiment of an electroplating process consists of four parts: (1) The external circuit, consisting of a source of direct current (Dc), means of conveying this current to the plating tank, and associated instruments such as ammeters, voltmeters, and means of regulating the voltage and current at their appropriate values. (2) The negative electrodes or cathodes, which are the material to be plated, called the work, along with means of positioning the work in the plating solution, so that contact made with the current source. (3) The plating solution itself, almost always aqueous, called by electrolyte the "bath"; (4) The positive electrodes, the anodes, usually of the metal being plated but sometimes of a conducting material which serves merely to complete the circuit, called inert or insoluble anodes. In order to achieve

Table 1. Chemical analysis of steel alloy 4130.

| Element | C | P | S | Mn | Si | Mo | Cr | Fe |
|------------|------|-------|------|------|------|------|-----|--------|
| Percentage | 0.31 | 0.035 | 0.04 | 0.55 | 0.32 | 0.17 | 0.9 | 97.675 |

a good adherence and performance to plated coat with a stirrer with constant speed, the plated specimen is prepared by using grinding paper ranged from 400-1000 till smoothing of surface, then sandblasted with Al_2O_3 Grade 80-120 using pressure 60 PSI for ensuring that the superficial is free from grease, then immersing in the pre-plating tank according to each type of coat, and followed by the plating tank containing salts of the plating material conforming with the type of coat (Nickel [Ni metal 75-90g/l-NiCl₂ 7.5g/l-Boric acid 30g/l] at 2 A/dm² and 25 °C, Copper [CuCl₂ 45g/l-NaCN 56g/l-Na₂CO₃ 30g/l-NaOH 7.5g/l] at 2 A/dm² and 50 °C and Cadmium [CdO 27g/l-NaCN 1.5g/l-NaOH 7.5g/l-Na₂CO₃ 7.5g/l] at 4 A/dm² and 50 °C) with an average coating thickness 20μ. All chemicals are purchased as pure chemical form certified supplier.

2.2.2. Electrochemical Measurements

2.2.2.1. Electrochemical Impedance Spectroscopy (EIS)

The electrochemical cell was a typical three electrode Pyrex glass cell at room temperature using a computer aided Autolabpotentiostat / galvanostat PGSTAT302N. A silver/silver chloride reference electrode ($E_o = 0.203$ V vs. SHE) was used as reference electrode, a platinum foil was used as the counter electrode, and the steel alloy 4130 was used as working electrodes in 3.5 % sodium chloride. Before each experiment, the open circuit potential (OCP) was recorded for at least 30 min. The ac frequency range extended from 0.1–10⁵ Hz. with a 10 mV peak-to-peak sine wave as the excitation signal. Electrochemical impedance spectra (EIS) were recorded at E_{corr} (i.e. at the stabilized OCP). All impedance data were fitted to an

appropriate equivalent circuit. The inhibition efficiency obtained from EIS measurements

$$IE\% = \frac{R_{ct} - R_{ct}^o}{R_{ct}} \times 100$$

Where, R_{ct} and R_{ct}^o are the charge transfer resistance in the uncoated and coated steel alloy 4130.

2.2.2.2. The Potentiodynamic Polarization Studies

The potentiodynamic polarization studies carried out in the same setup as that of electrochemical impedance studies. After electrochemical impedance measurements, polarization curves were recorded at scan rates of 1 mVs⁻¹ to study corrosion behavior of uncoated and coated samples. All the polarization measurements were performed in the potential range from the cathodic to the anodic side (-0.8 to 0.1 V) and at room temperature. The inhibition efficiency calculated using the Tafel extrapolation method, by using

$$IE\% = \frac{i_{corr} - i'_{corr}}{i_{corr}} \times 100$$

Where, i_{corr} and i'_{corr} are the corrosion current density in the uncoated and coated steel alloy 4130.

2.2.2.3 Cyclic Voltammetry:

Cyclic Voltammogram is obtained by measuring the current at the working electrode during the potential scans

2.3. Surface Examination

The surface morphology of the uncoated and coated steel alloy 4130 electrodes before and after immersion in 3.5% sodium chloride are

performed on scanning electron microscope (SEM, JOEL, JSM-T20, Japan). Three specimens of new leaded bronze alloy were used as the metal substrate; this alloy consists of (Cu = 76.5, Pb = 17.85, Sn = 2.68, As = 2.65 and Mn = 0.32).

3. Results and Discussion

3.1. Open Circuit Potential

The (OCP) open circuit potential of coated steel alloy 4130 with nickel, copper and / or cadmium is measured in 3.5 % NaCl. The acquired results are presented in Fig. 1. As mentioned in Fig. 1, the OCP values at the first 500 sec show that the Ni-coated steel alloy 4130 is the best corrosion resistance due to the shift towards the positive values. After the first 500 sec the OCP values have same magnitudes of uncoated steel alloy 4130 of about -543 mV notably the opposite behavior is achieved in case of Cu-coated steel alloy 4130, since the OCP values showed lower magnitudes compared with uncoated and Ni-coated steel alloy 4130. In addition, after 500 sec the Cu-coated steel shows higher magnitudes in OCP due to the formation of adsorbed intermediates from CuCl^- . The adsorbed intermediate form negative charges on the coated copper surface -504 mV [33-35]. This shift of OCP values to more negative regions is attributed with presence of high content of chloride ion concentration in the electrolyte [36, 37]. After the first 500 sec the OCP values shifted to the positive direction of about -526 mV and the surface became more corrosion resistance compared with the Ni-coated and the uncoated electrode. Finally, the Cd-coated electrode register the lowest corrosion resistance of the tested materials and the OCP shifted to the more

negative values of about -689 mV, and this value is indicating to the highest corrosion rate of this sample.

3.2. Potentiodynamic Polarization Results

For more illustration about the evaluation and investigation of the corrosion behavior of coated steel alloy 4130, potentiodynamic polarization measurements carried out. Fig. 2 illustrates the polarization curves of uncoated and coated steel alloy 4130 in 3.5 % NaCl solution. As can be seen from Fig. 2, the polarization curves shift to positive direction from cadmium, copper and nickel. The highest shift is achieved in case of Ni-coated steel alloy 4130 and decreasing from copper to cadmium. This behavior clearly noticed from the values of corrosion potential (E_{corr}) and can be observed according to the present parameters in Table 2. In addition, this trend proved by monitoring the corrosion current density, since it decreases from cadmium, copper and nickel, which points to decreasing the corrosion rate of steel alloy 4130. From the slope values of the anodic Tafel as seen in Table 2, it can be anticipated that the disbanding or degradation of steel alloy 4130 in saline solution is showed high corrosion rate compared with the coated samples, since the inhibition efficiency is gradually increase from cadmium, copper and nickel of about 56.9, 89.1 and 90.7. On the other hand, the polarization curves can provide the classification of investigated coated samples, since improve the inhibition of anodic and cathodic reaction, so we can consider these coated materials have the same behavior of mixed-type corrosion inhibitor system. However, the coated materials are meaningfully diminishes the current density

in both of the cathodic and the anodic regions if it overlaid with the uncoated steel alloy 4130 and the minimum percentage of inhibition efficiency was achieved in cadmium coated sample. As can be seen in Fig. 2, the coated materials have good coverage on the surface of steel alloy 4130, so the reaction sites are blocked, then decreases the contact between destructive ions and the steel surface.

3.3. Current Transients

Potentiostatic current transients were measured on uncoated and coated steel alloy 4130 electrodes in 3.5 % NaCl and the results are presented in Fig. 3. The results illustrate preliminary hurried increase of current with elapsed time previously the current inclines to level off near to the steady value. Afterward 30 min the current values were 83.5, 58.8, 36.7 and 17.1 mA cm⁻² for the uncoated, Cd-coated, Cu-coated, and Ni-coated respectively. An order of inhibition efficiency increases from cadmium, copper and nickel of about 29.5, 56 and 79.5%, respectively. This is an illustration of the remarkable efficiency of Ni-coated steel alloy 4130 against the corrosion inside the passive area. At these conditions, the protection or corrosion control is accredited with the development of good coat of nickel on the steel alloy 4130 and the reduction of current values with time is attributed with the advanced escalation of the inhibition efficiency of the protective layer of nickel with time of immersion. The steady state of current transients in the presence of nickel layer is about one and half fold greater than the current transients of copper layer and about two fold greater than the current transients of cadmium layer.

3.4. Polarization Resistance Results

The electrochemical impedance spectra were measured for uncoated and coated steel alloy 4130 and the gained results summarized in Fig. 4. Table 3 shows the obtained parameters after fitting the EIS data with the corresponding circuit presented in Fig. 5 for the uncoated and Ni-coated, Cu-coated and Cd-coated steel alloy 4130 in 3.5% NaCl solution at 298 K. The highest important item in these data is focusing on the polarization resistance (R_p). In point of view the analysis yields from the (R_p) values give clear indication about the tendency of corrosion process. However, the (R_p) values are inversely proportional to the corrosion rate and the relation can be summarized from the following equation:

$$R_p = \frac{K}{i_{corr}}$$

where K is a constant for each system.

These EIS experiments approved to explain the kinetic parameters between the steel alloy 4130 and saline solution interface in the absence and in the presence of coated layer. As seen in Fig. 4, the steel alloy 4130 in this saline solution shows semicircle that its diameter got bigger with the increase of the polarization resistance R_p depending on the kind of coat on the steel surface. This behavior indicates that the increase of R_p decreases the dissolution of steel alloy 4130 in salt solution and the EIS data simulated to fit the equivalent circuit Fig. 5 using ZSimpwin software and the obtained related data showed in Table 3. The equivalent circuit contains some electrochemical parameters. This equivalent circuit model used to fit the obtained EIS from evaluation the corrosion and corrosion inhibition of steel alloy 4130 in sodium chloride medium.

Fig. 1: Open circuit potential of coated steel alloy 4130 with Nickel, Copper and /or Cadmium in 3.5 % NaCl solution.

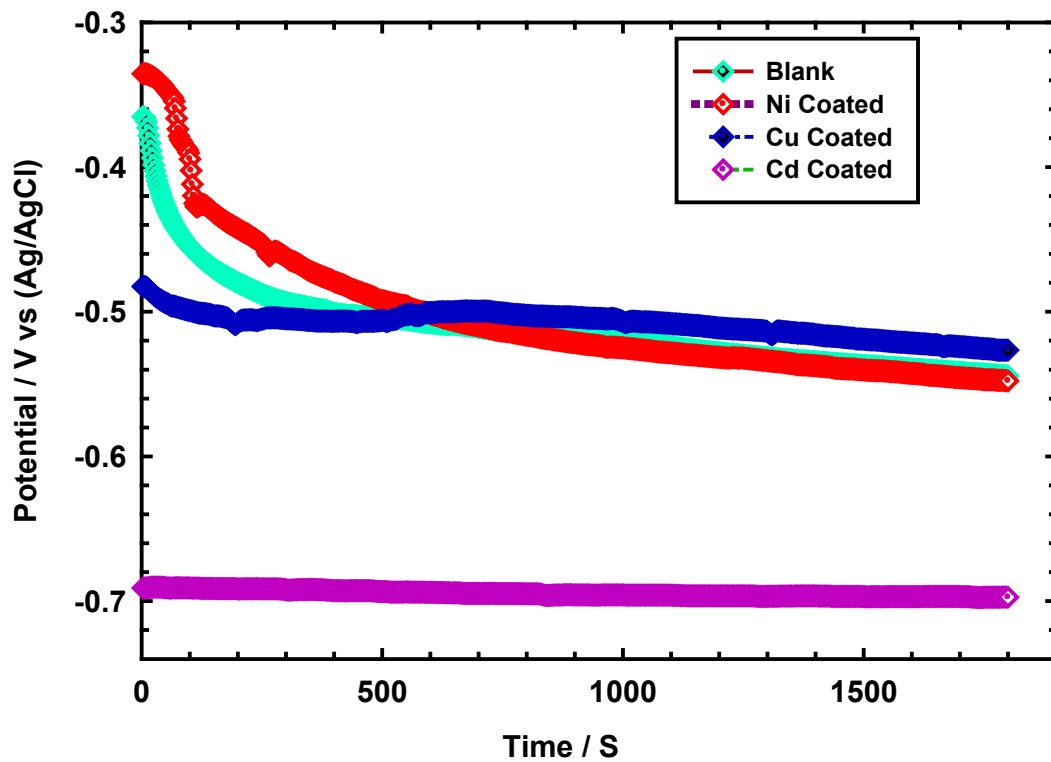


Fig. 2: Effect of choride ions on the potentiodynamic polarization curves of uncoated and nickel, copper and /or cadmium coated steel alloy 4130 at 298 K.

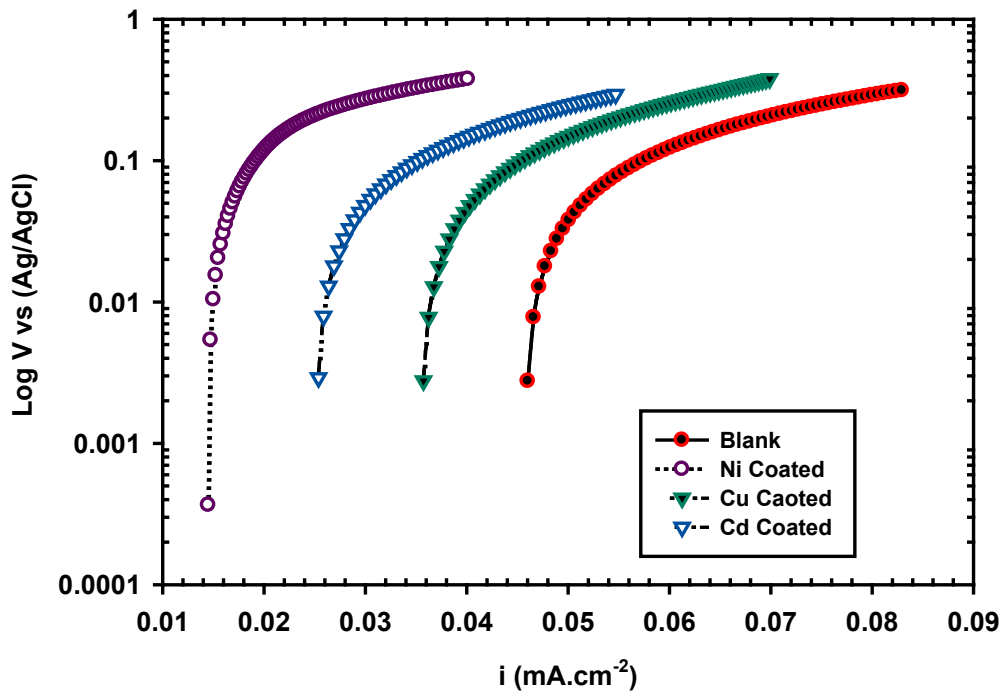


Table 2: Electrochemical parameters for un-coated and Ni-coated, Cu-coated and Cd-coated steel alloy 4130 in 3.5.% NaCl solution at 298 K.

| Coat type | B_a , mV/dec | B_c , mV/dec | I_{corr} , μA | E_{corr} , mV | C.R, mpy | IE, % |
|-----------|----------------|----------------|----------------------|-----------------|----------|-------|
| Uncoatd | 201.9 | 176.4 | 536.4 | -842.4 | 129.9 | ---- |
| Ni-coated | 378.1 | 254.2 | 55.1 | -718 | 12.67 | 90.2 |
| Cu-coated | 287.8 | 180.5 | 55.5 | -708.7 | 13.44 | 89.6 |
| Cd-coated | 277.2 | 185.9 | 256 | -992 | 62.11 | 52.2 |

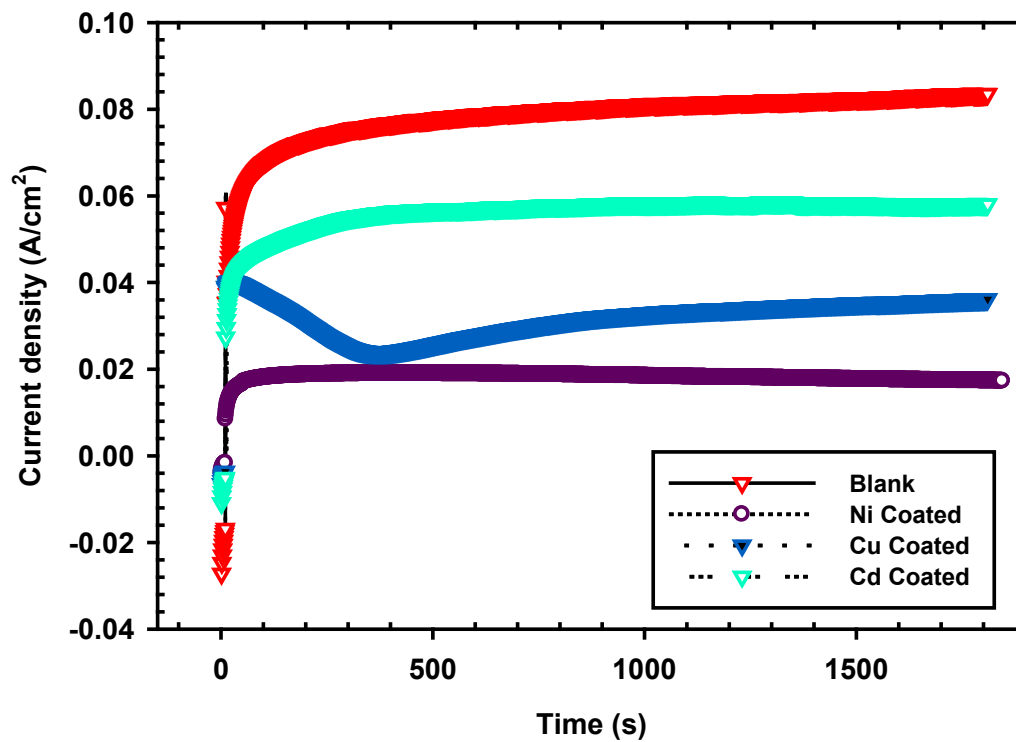
Fig. 3: Potentiostatic current transients of un-coated and Ni-coated, Cu-coated and Cd-coated steel alloy 4130 in 3.5.% NaCl solution at 298 K.

Fig. 4: Plots of (a) Nyquist impedance curves (b) impedance frequency relationship for the uncoated and Ni-coated, Cu-coated and Cd-coated steel alloy 4130 in 3.5.% NaCl solution at 298 K.

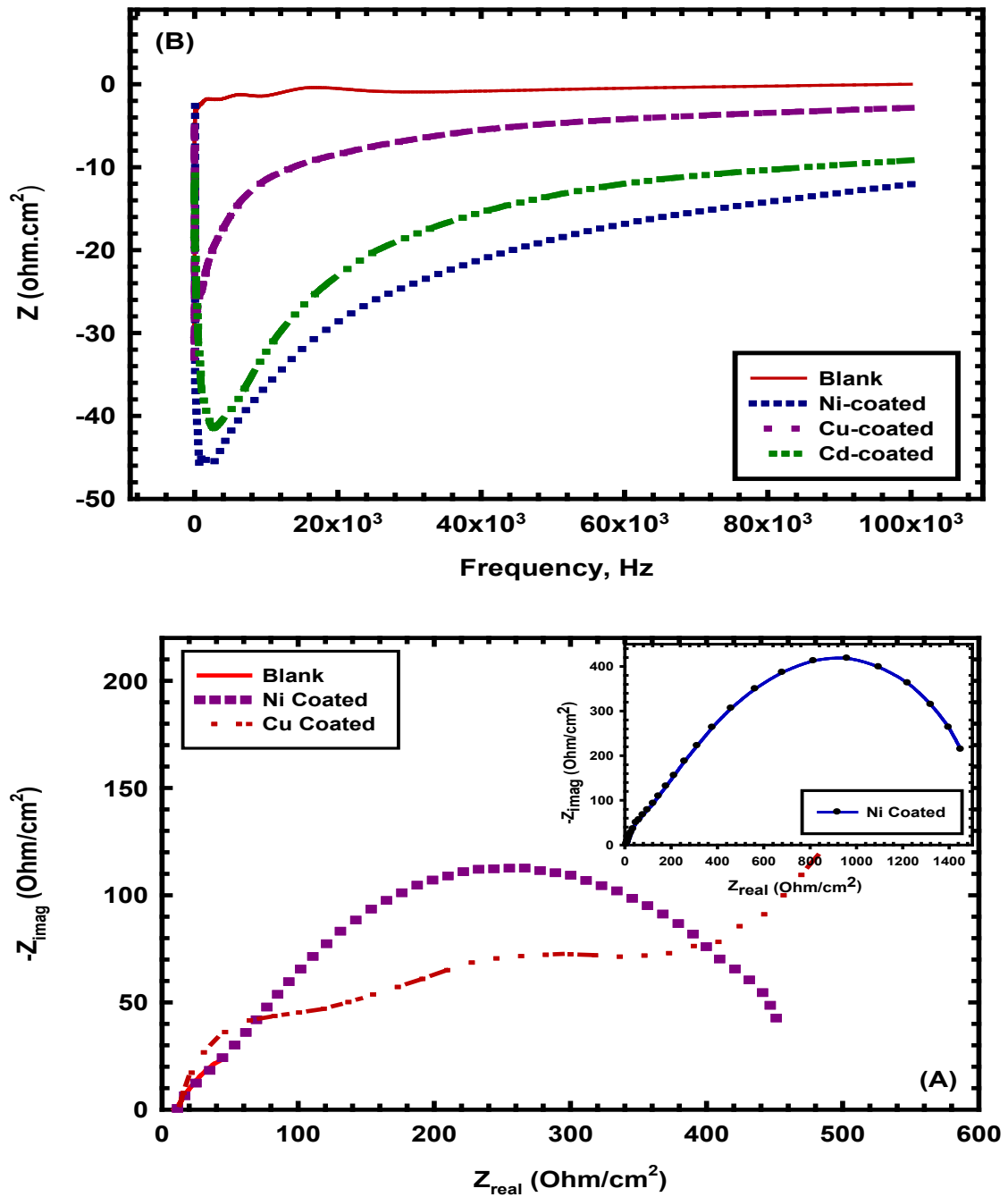


Table 3: Parameters obtained by fitting the EIS data with the equivalent circuit shown in Fig. 4 for the uncoated and Ni-coated, Cu-coated and Cd-coated steel alloy 4130 in 3.5.% NaCl solution at 298 K.

| Coat type | R_s, Ω | R_{cp}, Ω | R_p, Ω | C_{cd}, mF | n | C_c, mF | m |
|-----------|---------------|------------------|----------------------|-----------------------|-----------------------|-----------------------|-------|
| Blank | 9 | 154.8 | 1.106 | 0.07468 | 1.85×10^{-3} | 1.85×10^{-3} | 0.646 |
| Ni-coated | 4.709 | 1759 | 0.2938 | 2.36×10^{-4} | 0.5224 | 8.9×10^{-8} | 0.912 |
| Cu-coated | 9.747 | 548.7 | 5.5×10^{-2} | 1.47×10^{-4} | 4.2×10^{-9} | 4.2×10^{-9} | 0.804 |
| Cd-coated | 13 | 833.9 | 6.3×10^{-2} | 1.57×10^{-3} | 2.8×10^{-6} | 2.87×10^{-6} | 0.918 |

Fig. 5: The equivalent circuit model used to fit the EIS data obtained for the uncoated and nickel, copper and /or cadmium coated steel alloy 4130 in 3.5.% NaCl solution at 298 K.

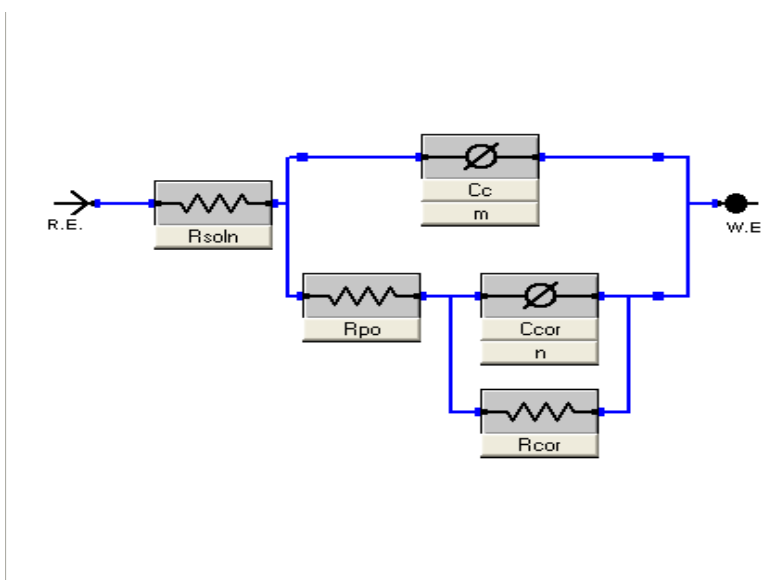
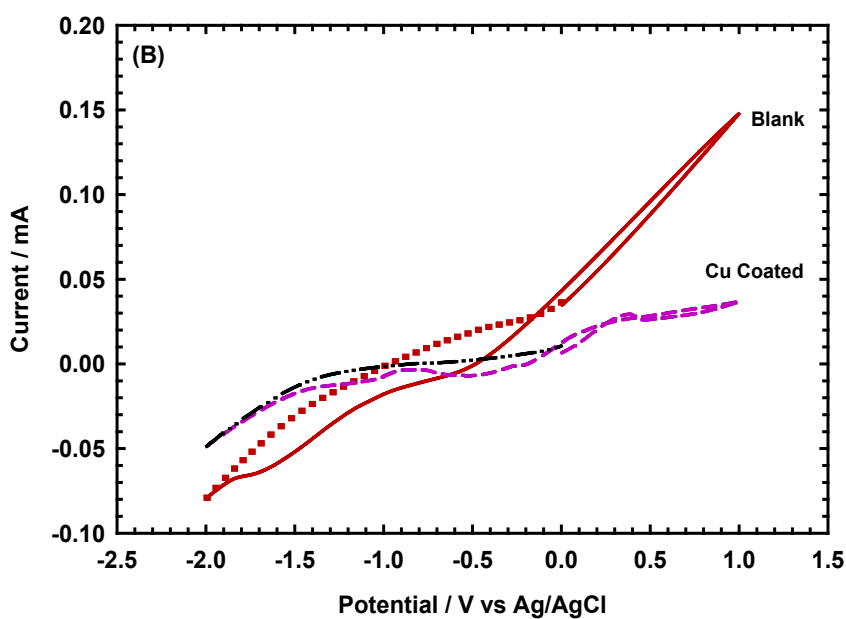
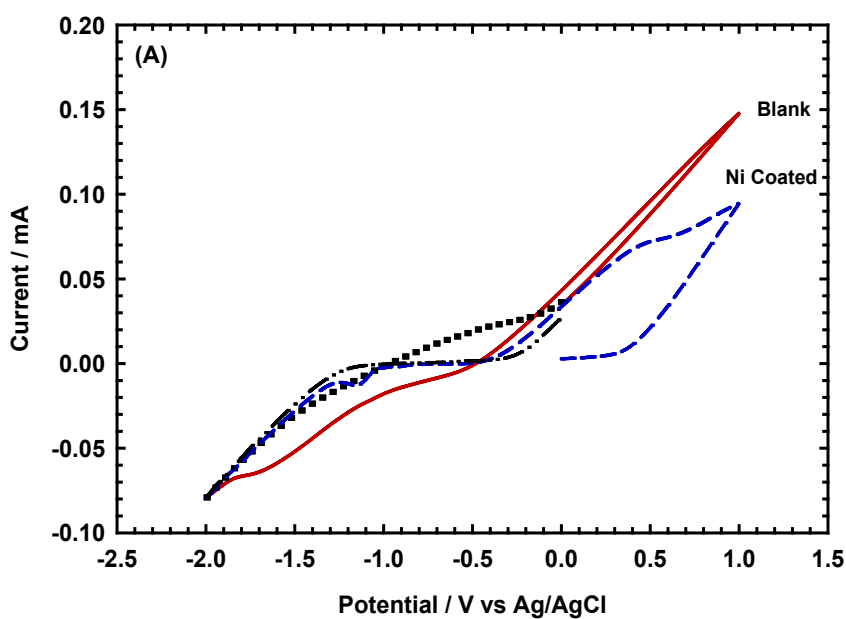


Fig. 6: Cyclic voltammety curves of un-coated and (a) Ni-coated, (b) Cu-coated and (c) Cd-coated steel alloy 4130 in 3.5.% NaCl solution at 298 K



However, R_{soln} represents the solution resistance, R_{po} is the polarization resistance for the solution/carbon steel interface, also defined as the charge transfer resistance, and ϕ is the inductance all of these values listed in Table 3.

3.5. Cyclic Voltammetry

The cyclic voltammogram of steel alloy 4130 in salt solution without and with nickel coat shown in Fig. 6a. The obtained CV curves of steel alloy 4130 in salt solution indicate that Fe undergoes oxidation to Fe^{++} ions. The Fe dissolution naturally occurred at the anode in saline solution through the formation of ferrous ions. In addition, the reduction process of the dissolved O_2 happens at the cathode and forming water molecules. The steel corrosion in salt solution is generally affected by presence the Cl^- ions by forming unstable ferrous chloride. This unstable compound has no ability to protect beneath surface of steel alloy 4130, so further dissolution occurred by reacting with more Cl^- ions and forming ferric chloride. The FeCl_3 is soluble in water so the corrosion process in chloride solution simultaneously process. Consequently, it clearly noticed from the piercing growth of the current density in cyclic voltammetry curves, which arguments to enhance the rate of corrosion of steel alloy 4130. The practical tests are repetitive in case of copper coated and cadmium coated steel alloy 4130 as seen in Fig. 6b and Fig. 6c respectively. The obtained CV curves confirmed that a protective effect observed in the presence Ni-layer more than the protection in Cu-layer but in case of Cd-layer is registered the lowest protective layer. These behaviors can be more explained from the corrosion current density and the anodic peak was not observed and the gradually decreases is clearly noticed. It proposed that

in saline solution, in the presence of Ni-layer and Cu-layer approaches to the presence of no weaknesses in the defensive layer compared with Cd-layer. Therefore, aggressive chloride ions become in interaction with the surface of steel alloy 4130, so steel degradation is sustained but with different rate depending on the kind of coating layer. It is well known that chloride ions can enter the defensive layer on the steel surface, which primes to localized attack specially pitting corrosion. This performance established that there is a weakening of the defending layer and pits develop always on the surface of steel alloy 4130. Consequently, there are also cathodic peaks demonstrating the reduction process of steel ions, and the strength of reduction peak diminished in the occurrence of Ni-layer and Cu-layer but increase in presence of Cd-layer. This suggests the resistivity effect of the Ni-layer and Cu-layer in the presence of chloride ions. The chloride ions penetration through the coated layer is back to the small diameter of chloride anions, which obviously noticed through the pitting corrosion.

3.6. Microstructure Characterization

3.6.1. Surface Characterization SEM

The scanning electron microscope (SEM) micrographs of the uncoated and coated steel alloy 4130 coupons before and after immersion in 3.5 % NaCl are presented in Figs. 7a-d and Figs. 8a-d. According to the analysis of SEM, it noticed that there has been no variation of uncoated steel alloy 4130 surface before corrosion experiment see Fig. 7a. After corrosion experiment with the 3.5 % NaCl the surface has a significant change specially the clear notably of localized

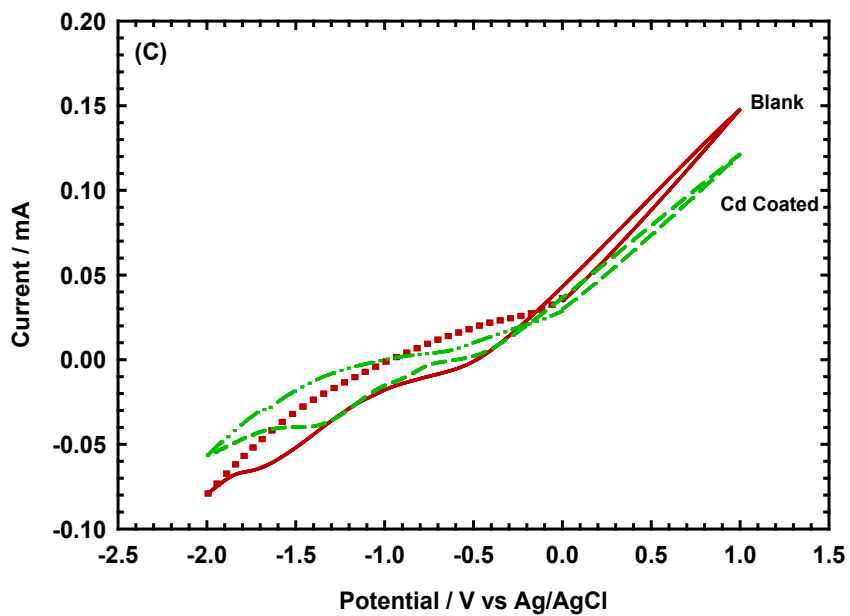
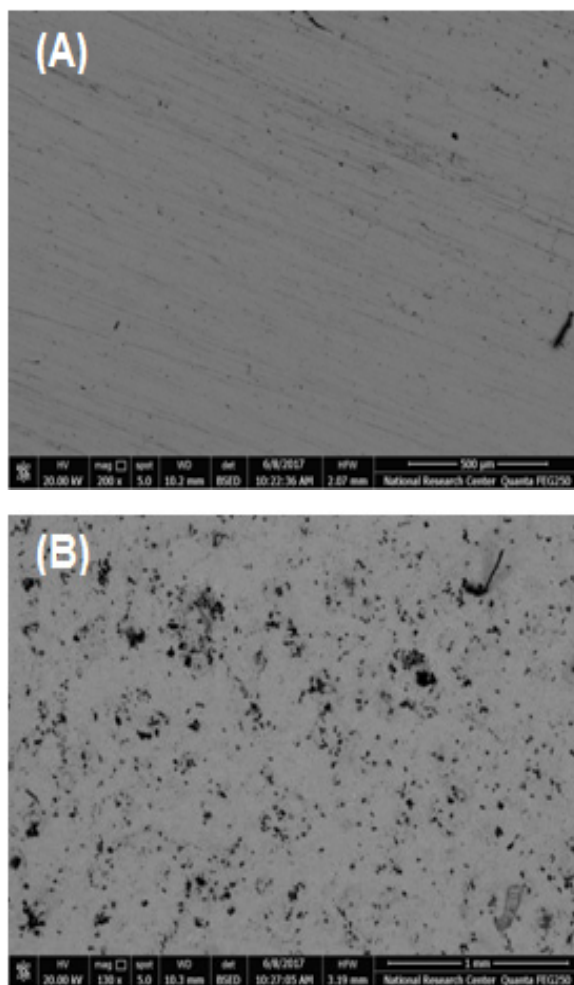
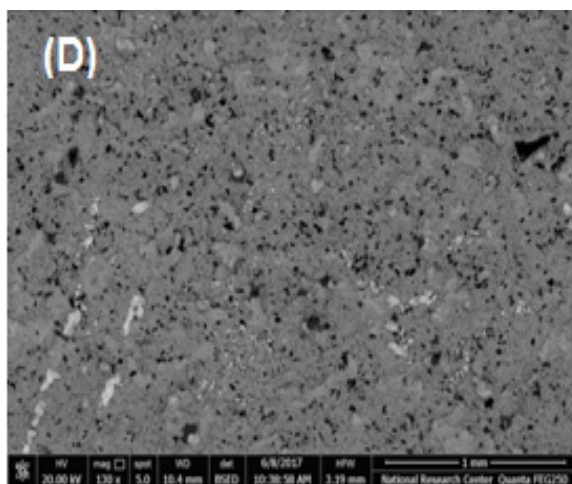
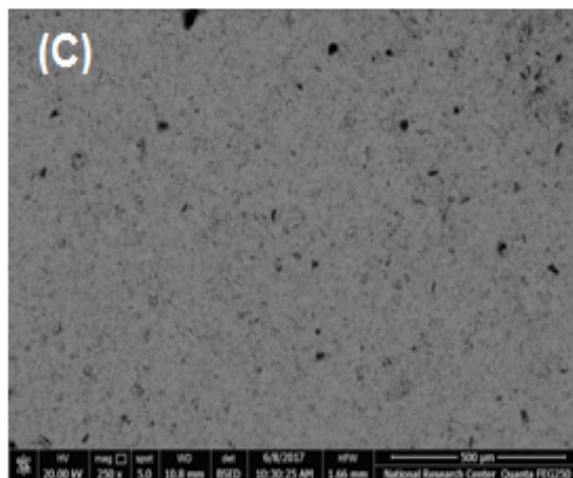


Fig. 7: Scanning electron microscopy images of (a) un-coated (b) Ni-coated, (c) Cu-coated and (d) Cd-coated steel alloy 4130 before immersion in 3.5.% NaCl solution.





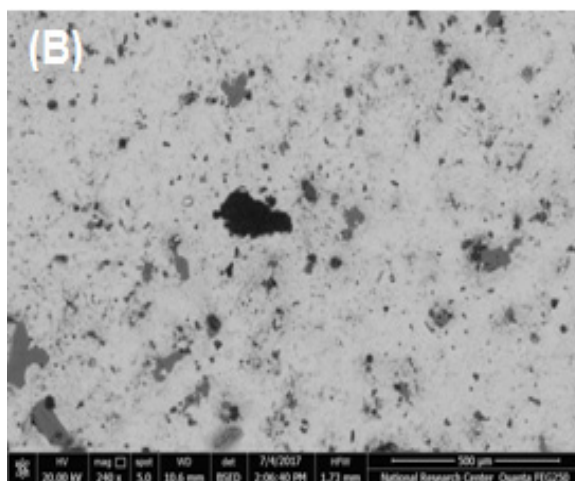
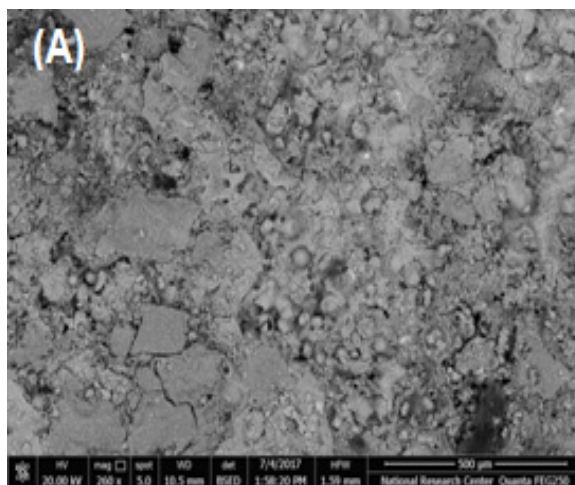
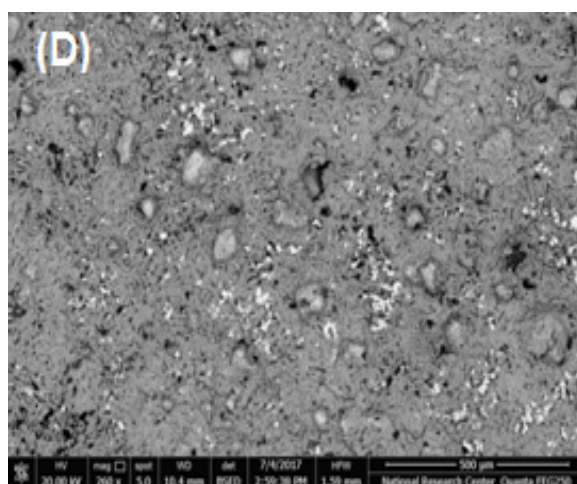
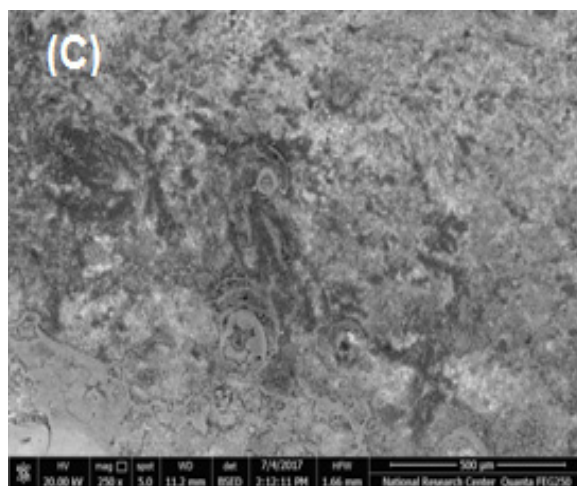


Fig. 8: Scanning electron microscopy images of (a) un-coated (b) Ni-coated, (c) Cu-coated and (d) Cd-coated steel alloy 4130 after immersion in 3.5.% NaCl solution.



corrosion and the surface of uncoated steel alloy 4130 demolished by destructive chloride attack see Fig. 8a. Though, in the occurrence of Ni-coated steel alloy 4130 before corrosion experiment (Fig. 7b), the surface is flatter and there is no corrosion product committed to the alloy surface. This authorizes that the outcome data of the minor corrosion rate in the existence of Ni-layer. After immersion in salt water, the surface suffers from some localized attack on the surface of Ni-layer see Fig. 8b. In case of Cu-layer, it noticed that there is no localized or general corrosion before the immersion in saline media as mentioned in Fig. 7c. In addition, after the immersion in salt water the surface affected by medium attack from the chloride ions and this behavior have been seen from the pitting corrosion in many sites on the Cu-layer see Fig. 8c. Finally, Cd-layer before corrosion experiment shows very smooth and clear surface, and it seen in Fig. 7d. After immersion of Cd-coated steel alloy in chloride solution, the surface destroyed by general and localized attack on the Cd-layer see Fig. 8d.

Conclusions

The corrosion behavior of uncoated and Ni, Cu and Cd coated steel alloy 4130 in 3.5 % NaCl have been investigated using electrochemical techniques. The obtained results from the electrochemical measurements are in good concurrence. Higher corrosion resistance clearly observed for the Ni-coated steel alloy compared with both Cu and Cd-coated samples. This behavior could be due to the stability and approximately perfect and spreading coat of Ni-layer. The surface characterization proved that the Ni-coated

has clean and smooth surface, but in case of Cu-coated sample, the surface shows corrosion products and observed destruction of surface. In case of Cd-coated sample, observed localized and general corrosion. Finally, we can conclude that the best sample is Ni-coated steel alloy 4130.

References

1. M. A. Hegazy, A. Y. El-etre, M. El-shafaie and K. M. Berry, (2016) *J. Mol. Liq.*, 214: 347–356.
2. H. Vashisht, I. Bahadur, S. Kumar, K. Bhrara, D. Ramjugernath and G. Singh, (2014) *Int. J. Electrochem. Sci.*, 9: 2896–2911.
3. G. Boisier, A. Lamure, N. P'eb'ere, N. Portail and M. Villatte, (2009) *Surf. Coat. Technol.*, 203: 3420–3426.
4. C. Jeyaprabha, S. Sathiyarayanan and G. Venkatachari, (2005) *J. Electroanal. Chem.*, 583: 232–240.
5. H. M. A. El-lateef, A. M. Abu-dief and B. E. M. El-gendy, (2015) *J. Electroanal. Chem.*, 758: 135–147.
6. M. A. Migahed, A. M. Abdul-Raheim, A. M. Atta and W. Brostow, (2010) *Mater. Chem. Phys.*, 121: 208–214.
7. J. Saranya, M. Sowmiya, P. Sounthari, K. Parameswari, S. Chitra and K. Senthilkumar, (2016) *J. Mol. Liq.*, 216: 42–52.
8. A. A. Farag, A. S. Ismail and M. A. Migahed, (2015) *J. Mol. Liq.*, 211: 915–923.
9. R. E. Ram'irez, L. C. Torres-Gonz'alez and E. M. S'anchez, (2007) *J.*

- Electrochem. Soc., 154: B229.
10. D. Mercier and M. G. Barth'es-Labrousse, (2009) *Corros. Sci.*, 51: 339–348.
 11. A. Popova, M. Christov and A. Zwetanova, (2007) *Corros. Sci.*, 49: 2131-2143.
 12. K. Bhrara and G. Singh, (2006) *Appl. Surf. Sci.*, 253: 846–853.
 13. Sudershan Kumar, Madhusudan Goyal, Hemlata Vashisht, Vandana Sharma, Indra Bahadur and Eno E. Ebenso, (2017) *RSC Adv.*, 7: 31907-31920.
 14. Mohammed A. Amin, M. A. Ahmed, H. A. Arida, Fatma Kandemirli, Murat Saracoglu, Taner Arslan, Murat A. Basaran, (2011) *Corr. Sci.* 53: 1895–1909.
 15. Kraka E., Cremer D., (2000) *J. Am. Chem. Soc.*, 122: 8245-8264.
 16. Awad M. K., (2004) *J. Electroanal Chem.*, 567: 219-225.
 17. Fang J. and Li J., J. (2002) *Mol. Struct. (Theochem)*, 593: 179-185.
 18. Arslan T., Kandemirli F., Ebenso E. E., Love I. and Alemu H., (2009) *Corros. Sci.*, 51: 35-47.
 19. K. F. Khaled, (2008) *Mat. Chem. & Phys.* 112: 290–300.
 20. G. Gece, (2008) *Corros. Sci.*, 50: (11), 1876-1878.
 21. Rodriguez-Valdez L., Martinez-Villafane A., and Glossman- Mitnik D., (2005) *J. Mol. Struct. (THEO CHEM)*, 716: 61-65.
 22. Lashkari M. and Arshadi M. R., (2004) *Chem. Phys.*, 299: 131-137.
 23. A. Zarrouk, B. Hammouti, R. Touzani, S.S. Al-Deyab, M. Zertoubi, A. Dafali, S. Elkadiri, (2011) *Int. J. Electrochem. Sci.*, 6: 4939.
 24. El-Sayed M. Sherif, Adel Taha Abbas, Hossam Halfa and A. M. El-Shamy, (2015) *Int. J. Electrochem. Sci.*, 10: 1777 – 1791.
 25. Wang H., Wang X., Wang H., Wang L., Liu A., (2007) *J. Mol. Model.*, 13: 147-153.
 26. B. Gomez, N. V. Likhanova, M. A. Dominguez-Aguilar, R. Martinez-Palou, A. Vela, J. Gasquez. (2006) *J. Phy. Chem., B*, 110: 8928-8934.
 27. A. A. Siaka; N. O. Eddy; S. Idris, L. Magaji, Res., (2011) *J. Appl. Sci.*, 6: (7-120), 487-493.
 28. Nnabuk O. Eddy, Stanislav R. Stoyanov and Eno. E. Ebenso, (2010) *Int. J. Electrochem. Sci.*, 5: 1127.
 29. Li Feng, Shengtao Zhang, Song Yan, Shenying Xu, Shijin Chen, (2017) *Int. J. Electrochem. Sci.*, 12: 1915-1928.
 30. M. A. J. Mazumder, H. A. Al-Muallem and S. A. Ali, (2015) *Corros. Sci.*, 90: 54.
 31. A. Pourghasemi Hanza, R. Naderi, E. Kowsari and M. Sayebani, (2016) *Corros. Sci.*, 107: 96.
 32. S. Cao, D. Liu, H. Ding, K. Peng, L. Yang, H. Lu and J. Gui, (2016) *J. Mol. Liq.*, 220: 63.
 33. X. Zheng, S. Zhang, W. Li, M. Gong and L. Yin, (2015) *Corros. Sci.*, 95: 168.
 34. M. Finsgar, (2013) *Corros. Sci.*, 72: 82-89.
 35. K.M. Ismail, (2007) *Electrochim. Acta*, 52: 7811-7819.

-
36. D. q. Zhang, Q. R. Cai, X. M. He, L. X. Gao, G. D. Zhao, G. D., (2008) Mater. Chem. Phys., 112: 353-358.
 37. Zaklina Z. Tasic, Marija B. PetrovicMihajlovic, Milan M. Antonijevic, (2016) J Mol. Liq., 222: 1-7.